JOURNAL OF MATERIALS SCIENCE 32 (1997) 835–849

Review
Fuel ash corrosion of boiler and superheater tubes

S. C. SRIVASTAVA, K. M. GODIWALLA
National Metallurgical Laboratory, Council of Scientific and Industrial Research, Jamshedpur-831007, India

M. K. BANERJEE
Department of Chemistry, Regional Institute of Technology, Jamshedpur-831009, India

The scientific pursuit of the determination of mechanisms of corrosion of metals and alloys operating at high temperatures in thermal power generating environments has resulted in volumes of reported data, yet little achievement has been made so far. In reviewing the literature, it has been attempted here to indicate the diversified nature of the problems and the characteristics of various parameters such as mineralogical constituents of the fuel, fuel ash and various products of combustion (e.g. sulphurous oxides, sulphates, pyrosulphates, sulphides, etc.) in monitoring the rate of reactions, and hence corrosion, of component materials. Rapid and intensive corrosion attack due to conjoint action of gaseous, chemical and liquid phases under normal boiler operating conditions have been expressed to offer a really challenging situation for further studies.

1. Introduction

The fuel ash corrosion of boilers and super-heater tubes is a matter of great concern since it affects the performance of thermal power stations by lowering their efficiency to significantly below the anticipated level. The dangers of corrosion, in a conventional steam power plant, limit the temperature of the super-heat and the recovery of low grade energy from the flue gases; this usually prevents any further gain in thermodynamic efficiency of the system [1–3].

The first part of the problem relates to mass and energy transfer during the continuous combustion of the coal particles which produces oxides of sulphur and iron by the reactions:

$$FeS_2 \rightarrow FeS \rightarrow FeO(\& Fe_3O_4) + SO_2 \quad (1)$$

$$SO_2 + O \rightarrow SO_3 \leftrightarrows SO_2 + 1/2O_2 \quad (2)$$

and also vaporizes alkali metals from the fuels, and affects the gas phase reactions of alkali metals with chlorides and sulphates. The second part of the problem is related to the deposition and adhesion of ash particles and other deposits constituents on tubes under conditions of heat transfer; condensation and the interactions of volatile components during deposit formation; the effects of temperature gradients in fireside deposits and segregation of deposit constituents; the mechanism of complex reaction schemes [e.g. $K_3Fe(SO_4)_3$] and the electrochemical reaction sequence of molten fused salts with the alloy constituents of the constructional materials.

Meier *et al.* [4] have discussed the various mechanisms of high temperature oxidation of metals. They discussed effects due to specimen-shape, thermal cycling, multiple oxidant gases, gas velocity and erosion. Extensive work has been carried out by Narita *et al.* [5–9], on the sulphidation of iron based alloys. These studies indicate that sulphidation kinetics are several orders of magnitude higher than oxidation rates because of the higher diffusivity of sulphides. This degration, coupled with internal sulphidation, has been observed in nickel-containing alloys in aggressive environments comprising several different oxidants.

Several studies on iron are reported in the literature [10–16]. It has been observed that the oxidation rate of iron at 1173 K in a mixture of water vapour and hydrogen follow parabolic kinetics. If mechanical defects are made in the FeO scale on the surface and the specimen is then re-heated in a vacuum, lateral transport of FeO produces a thin layer of fine grained FeO over the exposed iron. In the presence of a temperature gradient, as is encountered in heat exchangers, turbine blades and other high temperature components, the extent of mass transport of FeO was somewhat larger with FeO grain size in the flaw area. The mechanism of transport is believed to be either surface or bulk diffusion of Fe^{++} ions.

Despite these efforts, problems of external corrosion and deposits remain troublesome in both boilers and gas turbines and are likely to continue to pose operational difficulties in the years ahead. The situation is further complicated because of the fact that corrosion

0022–2461

research conducted in operating boilers (or gas turbines) usually lead to disappointing results. Metal and gas temperatures and the composition of the flue gases and deposits in corrosion areas are difficult to determine accurately. In addition these conditions cannot be kept constant because of the normal variations in fuel characteristics such that the environment is constantly changing throughout the area where corrosion occurs. Also, the extent of corrosion can be measured only during outages, so that it is often impossible to identify the operating conditions directly responsible for metal losses.

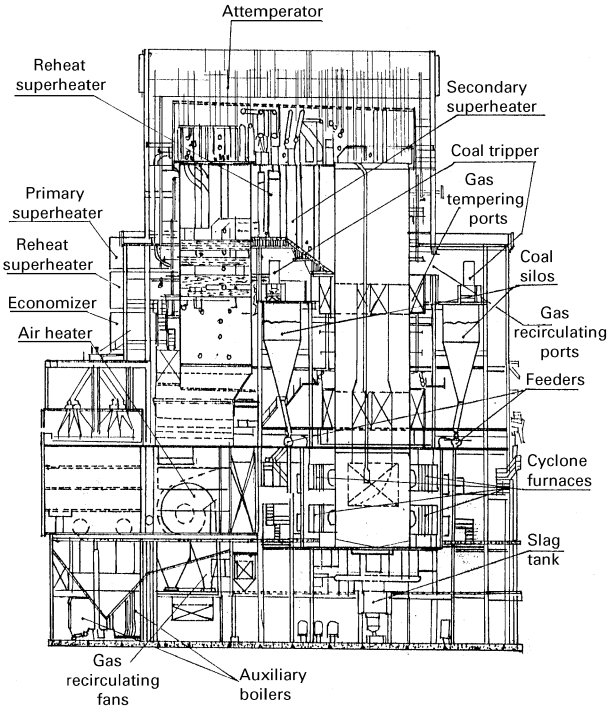

Figure 1 Schematic of a Universal Pressure Boiler, Coal-fired, with pressurized cyclone furnace. [Ref: Mechanical Engineers' Handbook, 9th edn, 1987, ed. by E. A. Avallone and T. Baumelster]

As a natural consequence, most of the proposed mechanisms of corrosion in combustion systems are based on laboratory investigations, where conditions in full-scale equipment can be partially duplicated. Although such attempts inevitably lack agreement their real significance rests on the interpretation of results; yet until better field installation measurements are possible, laboratory studies with all their shortcomings will continue to supply the knowledge of the steps by which corrosion takes place. These problems have been under investigation for many years and the results are extensively recorded in the literature.

In the present text, we attempted to produce a brief but descriptive picture of the problems of high temperature attack on metals and alloys under boiler operating conditions. We review the problem of high temperature corrosion in power plants and the mechanisms of reactions in various zones of the boiler and associated equipment.

A typical schematic diagram of a coal-fired steam power plant is depicted in Fig. 1. Fig. 2, shows a schematic of the various temperature zones in a commercial boiler.

2. Role of impurities

2.1. Moisture

Moisture, as an impurity in coal, is present chemically combined as water of hydration in some of the mineral impurities (notably the silicate minerals) and physically combined within the pore structure and on the surface of the coal. These can be driven off by heating the coal to a temperature of 378–383 K. This moisture from the coal remains in the coal/air mixture which is carried to the burners. The nitrogen present in the air acts as a diluent for reducing the flame temperature and increases the amount of heat carried out of the system by the waste flue gases.

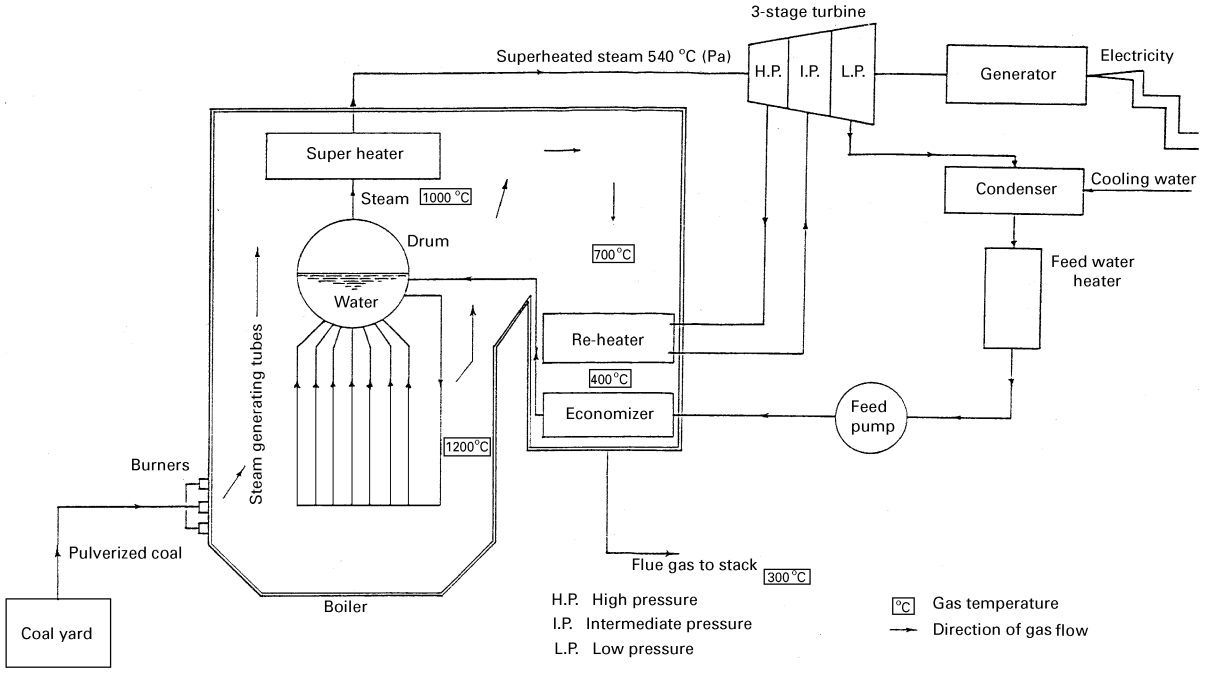

Figure 2 Schematic diagram of a typical modern coal-fired steam power station.

TABLE I Occurrence of minerals in coal

Mineral	Formula
Shale group	$(K, Na, H_3O_3, Ca)_2$ $(Al, Mg, Fe, Ti)_4$ $(Al, Si)_8O_{20}(OH, F)_4$ Al_2O_3–$2SiO_2$–$2H_2O$
Sulphur group	FeS_2–$FeSO_4$, Na_2SO_4
Carbonate group associated minerals	$CaCO_3$, $CaCO_3$–$MgCO_3$
Quartz	SiO_2
Feldspar	$(K, Na)_2O$–Al_2O_3–$6SiO_2$
Garnet	$3CaO$–Al_2O_3–$3SiO_2$
Hornblende	CaO–$3FeO$–$4SiO_2$
Gypsum	$CaSO_4$–$2H_2O$
Apatite	$9CaO$–$3P_2O_5$–CaF_2
Zircon	$ZrSiO_2$
Epidote	$4CaO$–$3Al_2O_3$–$6SiO_2$–H_2O
Biotite	K_2O–MgO–Al_2O_3–$3SiO_2$–H_2O
Aryite	CaO–MgO–$2SiO_2$
Pnochlorite	$2FeO$–$2MgO$–Al_2O_3–$2SiO_2$–$2H_2O$
Diaspore	$Al_2O_3 \cdot H_2O$
Lepidocrocite	$Fe_2O_3 \cdot H_2O$
Magnetite	Fe_3O_4
Kyanite	Al_2O_3–SiO_2
Staurolite	$2FeO$–$5Al_2O_3$–$4SiO_2$–H_2O
Topaz	$(Al, F)_2SiO_4$
Tourmaline	$MgAl_3(BOH)_2Si_4O_{19}$
Hematite	Fe_2O_3
Penninite	$5MgO$–Al_2O_3–$3SiO_2$–$2H_2O$

2.2. Ash

The high temperature chemical reactions of minerals are complex in themselves and are influenced by the presence of other substances during combustion. In the present state of knowledge, the properties of a coal ash can therefore be predicted from a knowledge of the mineral constituents of the coal (Table 1). The main metallic elements are aluminium, iron, calcium, magnesium, titanium, sodium and potassium. There is an appreciable body of literature on the sulphide, carbonate and chloride contents present in coals. The average ash analysis [17] of the coal found so far shows the presence of:

SiO_2 55–60%; TiO_2, P_2O_5, CaO, MgO about 1% each

Al_2O_3 20–30%; SO_3 as 0.2% and alkalis by difference about 1%

Fe_2O_3 10–15%

The behaviour in combustion of the complex moisture of inorganic materials in coal, depends not only on the nature and amount of the individual constituents, but also on the rate of heating and the maximum temperature reached. For example, the structure of layered shales breaks down at about 1273 K and melts completely at higher temperatures [18]. Kaolins also have a layered structure, and the effect of heat on them is similar to that on the shales.

The sulphides, kyanites and marcasite, begin to decompose [19] at 573 K. Under oxidizing conditions, the evolved sulphur is ultimately burnt to SO_2, but a proportion of the sulphur may be emitted as H_2S (at a temperature of 1273 K) in the flue gases, while some is retained as sulphides in the ashes. In a reducing or mildly oxidizing atmosphere, the reaction proceeds quantitatively to FeS, but in a fully oxidizing atmosphere, such as in pulvarized fuel firing, oxidation to ferric oxide (Fe_2O_3) occurs, possibly via $FeSO_4$, which has been detected at an intermediate stage. The oxides of magnesium and calcium formed due to the decomposition of various carbonates at temperatures in the range 773–1123 K react with ferrous sulphide (arising from the decomposition of pyrites and marcassite) to yield metallic iron under reducing conditions. Under oxidizing conditions, however, the oxides react with SO_2 to form sulphates which do not decompose until 1273 K [20–25].

The chlorides consist principally of sodium chloride with much smaller amounts of potassium, calcium and magnesium chlorides in the coals. The chloride ions appear to be released to a greater extent than the sodium ions under hot conditions. Fluorapatite, which is responsible for both fluorine and phosphorus impurities, readily loses fluorine leaving a residual complex calcium phosphate, which is a refractory material. Under reducing conditions it begins to lose phosphorus above 1753 K. In semi-reducing conditions, vaporization of phosphorus takes place at a temperature of 1873 K [26].

2.2.1. Loss on combustion efficiency due to ash, clinker and slag

The iron content of coal ash has a significant effect on the behaviour of ashes. Thus, when present in a completely oxidized form it raises the fusion temperature of the ash and in a less oxidized form it tends to lower the fusion temperature. The iron content and its degree of oxidation also have a significant effect on the ash viscosity which increases with ferrite content. Liquid slag is not troublesome as long as its viscosity is less than 25 PaS and it remains in liquid form. The most troublesome form is α-plastic slag which is arbitrarily defined to exist in the region where the viscosity is between 25–1000 PaS.

The presence of ash deleteriously affects the thermal efficiency of the boiler. Smaller boiler plants lose a significant amount of output if the ash is not removed continuously. However, a minimum ash content is also necessary for the formation of a protective layer over the fire-bars to prevent damage by over-heating. Clinkers formed on the side walls adjacent to travelling grates are invariably a nuisance. The phenomenon of clinkering and slagging of the inorganic constituents of coal is largely due to the result of complex chemical reactions – when molten slag from fire ash and fuel particles is blown out of the bed on the walls, or when the bed comes in contact with the refractories.

2.3. Sulphur and the sulphates

Sulphur leads to both high temperature corrosion when complex sulphates are involved, and to low-temperature corrosion caused by SO_3 condensing to form sulphuric acid (acidic fluxing) [27–30]. The compounds of sulphur with iron, oxygen and alkalis are mainly responsible for corrosion and accumulation of

deposits. The deposits in coal fired superheaters invariably show large quantities of sulphates and are often accompanied by 30–50% sulphur reported as SO_3. In the cold end of boilers (the flue), condensation of sulphuric acid limits the lowest safe metal temperature. Sulphur thus contributes to problems of corrosion and deposition when solid or liquid fuels are burned, either by itself as SO_3 or in conjunction with the alkali metals and other metals in the form of a wide variety of sulphates.

The two principal oxides, SO_2 and SO_3, present in the products of combustion of sulphur, react further to form sulphites, sulphates and complex pyrosulphates and trisulphates, which are involved in various corrosion processes. The overall reaction

$$H_2S + 3/2O_2 \rightarrow H_2O + SO_2 \quad (3)$$

scarcely suggests the actual complexity of the many intermediate reactions involved as shown in Table II [31]. Many of these reactions play no major role in the oxidation of sulphur, but in any study of chain-branching reactions, each possible reaction may influence the equilibrium concentration of the reactants or affect the total reaction rate.

It is also important to recognize that any source of sulphur (like FeS) would suffice and hence most of the total reaction mechanism does not depend on the initial presence of H_2S. Combustion in an excess of air converts the major portion of the sulphur into SO_2. Further reactions within the flames and oxidation of SO_2 is the main cause of occurrences of SO_3 in flue gas. The maximum amount of SO_3 that can be formed during the oxidation of SO_2 depends mainly on the temperature, with high equilibrium levels of SO_3 favoured at lower temperatures. Below 699 K, essentially all the sulphur in the system SO_2–SO_3 changes to SO_3 at equilibrium, whereas at about 1366 K it remains mainly as SO_2.

A better insight into the reaction mechanism can be gained by considering the phase stability which indicates the concentrations of minority species in Na_2SO_4 (e.g. O^{2-}, O_2^-, O_2^{2-}, $S_2O_7^{2-}$, SO_3^{2-}) and the stability of Na_2SO_4 itself, as functions of the oxygen and sulphur chemical potentials. Rapp and Goto [33] proposed that if the gradient of solubility of potential oxides with distance into the salt layer was negative at the oxide/salt interface, accelerated corrosion could be sustained.

TABLE II Reactions involved in the oxidation of sulphur

$H_2S \rightarrow SH + H - 91$ k.cal
$H + H_2S \rightleftarrows SH + H_2 + 19$ k.cal
$SH + O_2 \leftrightarrows SO + OH + 16$ k.cal
$OH + H_2S \leftrightarrows H_2O + SH + 22$ k.cal
$SO + O_2 \leftrightarrows SO_2 + O + 18$ k.cal
$O + H_2S \leftrightarrows OH + SH + 19$ k.cal
$SO + O \rightarrow SO_2$
$SO + SO \leftrightarrows S_2O_2 + 49$ k.cal
$SH + SH \leftrightarrows H_2 + S_2 + 26$ k.cal
$4S_2 \leftrightarrows S_8$
$SH + OH \leftrightarrows H_2O + S + 27$ k.cal
$S + O \leftrightarrows SO$
$S + S \leftrightarrows S_2$
$H + O_2 \leftrightarrows OH + O - 16$ k.cal
$O + H_2 \leftrightarrows OH + H - 2$ k.cal
$OH + H_2 \leftrightarrows H_2O + H + 15$ k.cal
$SO_2 + O + M \leftrightarrows SO_3 + M + 82$ k.cal
$SO + O_2 + M \leftrightarrows SO_3 + M + 93$ k.cal
$SO_2 + H_2 \leftrightarrows SO_2 + H_2O + 38$ k.cal

TABLE III Melting points of trisulphates and some related compounds formed from alkali sulphates

Compounds		Melting Point (K)
$K_3Fe(SO_4)_3$	···	891
$K_3Al(SO_4)_3$	···	927
$KFe(SO_4)_3$	···	967
$Na_3Fe(SO_4)_3$	···	897
$Na_3Al(SO_4)_3$	···	919
$NaFe(SO_4)_3$	···	963

2.4. Pyrosulphates

The failure of wall tubes and superheaters has been frequently blamed on alkali-pyrosulphates ($Na_2S_2O_7$ and $K_2S_2O_7$) which have a high chemical activity towards metal [33, 34]. While sulphates are implicated in providing a molten film on moderate to high temperature metallic surfaces, causing eventually metal wastage and corrosion; the pyrosulphate ($K_2S_2O_7$) exists in boiler furnaces only at temperatures upto about 783 K and $Na_2S_2O_7$ upto about 673 K. Neither of these compounds is likely to exist as deposits on superheaters where there is insufficient SO_3.

2.5. Alkali-iron trisulphates

The alkali-iron trisulphates [$Na_3Fe(SO_4)_3$ and $K_3Fe(SO_4)_3$] melt in the range of the super heater metal temperatures and they have been found to appear in corrosion areas. The overall reaction of the formation of trisulphates is:

$$3K_2SO_4 + Fe_2O_3 + 3SO_3 \rightarrow 2K_3Fe(SO_4)_3 \quad (4)$$

Table III, lists the melting points of the trisulphates along with several related compounds formed from alkali sulphates [36]. Again, these compounds are unlikely to sum at low SO_3 pressures.

3. Corrosion and deposits

Boiler manufacturers base their selection of alloys for high temperature service on oxidation and hot corrosion resistance data as well as on the mechanical properties of the steel which are listed in Table IV [37].

Combustion gases can cause high temperature oxidation and also hot corrosion in various other forms at many locations in boilers and gas turbines [38, 39]. The factors responsible are: (i) the composition of the original mineral constituents in coal, (ii) their size and distribution in the coal, (iii) the rate at which heating occurs, (iv) the mixing of the inorganics during combustion, (v) the maximum temperature, (vi) the time

TABLE IV Oxidation-resistant alloys superheater service

Material	ASTM Designation	Maximum metal temperature (K)	
		Recommended use	Oxidation limiting
Carbon steel	A 178 C, A 210	783	838
Carbon–0.5 Mo	A 209, T1A	797	838
0.5 Cr–0.5 Mo	A 213, T2	797	852
1.25 Cr–0.5 Mo	A 213, T11	838	866
2 Cr–0.5 Mo	A 213, T36	855	894
2.25 Cr–1 Mo	A 213, T22	880	908
5 Cr–0.5 Mo	A 213 TS	894	922
9 Cr–1 Mo	A 213, T 9	922	977
18 Cr–8 Ni	A 213, TP 304	1033	1144
16 Cr–13 Ni–3 Mo	A 213, TP 316	1033	1144

and turbulence while the ash constituents are in the gas stream, (vii) the atmosphere over the ash and (viii) the total time-temperature history of the ash-particles in the combustor.

All these factors affect the resultant corrosion. A moderate to high combustion rate leads to a liquid phase of melted pyrites (FeS), whereas a lower heating rate oxidizes the pyrites to Fe_2O_3, which later flux the silicates in the ash. Evidently, at zones where the gas temperature is above 811 K (as is the case with furnace wall tubes, superheaters, reheaters and economizers) high temperature corrosion attack is generally observed and where the gas temperature is less than 811 K (as is the case with air heaters and in stacks) metal loss occurs by "low temperature" corrosion.

Fig. 3 illustrates the effect of various atmospheres on the rate of oxidation of a low-carbon steel for an exposure period of 24 h [40]. For instance, at 1144 K steam, oxygen and air, oxidize the steel at about the same rate; the rate with SO_2 is about three times greater and at lower temperature (e.g., 922 K) the rate of oxidation markedly decreases indicating a penetration level of 13 mm per year in SO_2 and 8 mm in air. In an experiment [41] in which a large number of alloys were exposed to simulated flue gases at 1005 K, increasing the SO_2 content from 0.02–0.2 wt% roughly doubled the metal loss.

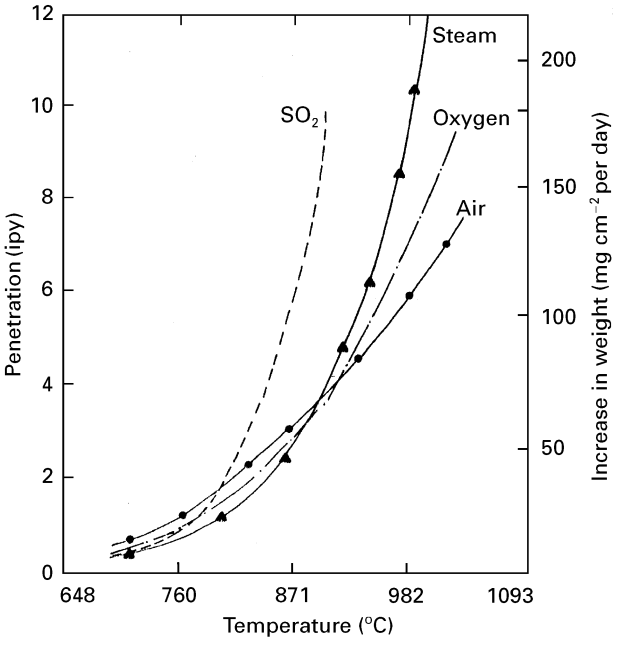

Figure 3 Effects of various atmospheres on the rate of oxidation of a low-carbon steel [66].

3.1. Boiler furnace

On a cooled target, the deposition of flue gas containing sulphates is proportional to the difference between the partial pressure of the species in the gas and that at the deposit surface [42, 43]. The mechanism of the deposition of flue gas-borne ash on boiler tubes is difficult to predict due to the uncertain temperature gradient. During initial stages of deposit formation, when the surface temperature of a clean boiler tube is around 700 K, the thermophoresic deposition of small particles (less than 5 μm in diameter) may build up slowly. This layer has a low thermal conductance and so the surface temperature increases sharply.

The overall mechanism of deposition of ash constituents of the flue gas on the cooled boiler tube may be due to a combined effect of the following:

(i) deposition of sulphates by vapour deposition process;
(ii) deposition by particle diffusion;
(iii) thermophoresic and electrophoresic deposition; and
(iv) through a process called inertial impaction when the stream velocity is high.

Failure of the links of chain-gate stokers and of wall tubes near the fuel is mainly because of overheating of the grates due to the local obstruction of the air flow by clinkering of the sticky particles in the fuel bed. Peak metal temperatures as high as 1311 K are observed with full-burning coal, whereas coking coals under the same test conditions lead to metal temperatures no higher than 833 K. This indicates that the nature of the fuel bed radically affects the temperature of metal parts, and that any unprotected stoker section, exposed to areas of the fuel bed where combustion is occurring, can easily be heated up to temperatures approaching 1366 K.

Since the reaction between coal-ash slag and other solids at temperatures below about 1477 K are considered to be extremely unlikely, except in the case of highly reactive fluxes such as limestone, salt cake, or fluorspar, the effect of ash, as noted above is mainly physical i.e., prevention of normal air flow through stoker parts and over-heating. However, chemical reactions can occur, for instance, between iron stoker parts and iron pyrites or marcasite, FeS_2; these inorganic sulphides dissociate at temperatures between 533–817 K to form FeS which in turn, can lead to rapid corrosion of iron at quite moderate temperatures. As can be observed from Fig. 4, iron can react with FeS to form an α-eutectic which melts at 1258 K, and that FeO and FeS form a eutectic melting at 1213 K, both of these eutectics are liquids in the range of metal temperatures of grate bars and tuyeres. It is because of this reason that rapid metal loss can be expected. The FeS produced from pyrites and marcasites is unlikely to be oxidized to Fe_2O_3 as readily in a zone of blocked air flow as when the fuel bed is relatively open. Hence clinkers formed on grates are doubly problematic; firstly, by raising the temperature of the metal parts, and secondly, by encouraging the presence of FeS at temperatures where it is easily capable of damaging iron parts.

The loss of metal from the lower parts of tubes in the sidewalls of stoker-fired furnaces has also been troublesome. In this case erosion by the moving fuel bed is found to occur, particularly as a result of FeS attack.

Deposits may also cause problems by the plugging of gas passages. Such deposits often collect on the alkali-matrix bases formed when sodium and potassium are volatilized in the flame, condense on relatively cool boiler and superheater tubes and then react with SO_2 and O_2 or with SO_3 to form sticky surfaces. Usually, this matrix base contains large amounts of alkali sulphates to which particles of ash are suspended and bonded to form an adherent deposit.

3.2. Superheaters

Corrosion of superheaters poses a major problem in the operation of coal and oil-fired steam generators and no simple means has been found for its elimination. Selecting the most economical superheater alloy for a given application requires compromises established by the working pressure and the temperature, as well as by the fabrication characteristics of the alloy. Carbon steel is considered to be the most economical below 6205 kPa and 783 K, while low-alloy steels with up to 3 wt% chromium are usually adequate at temperatures ranging upto 880 K. Above this temperature, much more chromium should be present and, in the highest duty alloys, an appreciable percentage of nickel is also required to produce an austenitic alloy. In the case of the austenitic 18Cr–8Ni alloy series, the temperature limit depends on the presence or absence of sulphur and vanadium. Sulphates on the surface of ferritic steels of 2.25Cr–1Mo and austenite steels of 18Cr–12Ni–1Mo have little effect on the oxidation rate of the metal in air at temperatures up to about. 977 K. Chlorides, however, increase oxidation above 672 K, presumably by destroying the protective layer of chromium-iron spinel on the outer surface of austenitic steels. When alkalis are present, chromium is lost from the surface as volatile chromium chloride, increasing the oxidation rate to replace the normal chromic oxide film. A typical example of deposits and corrosion on a reheater element is shown in Fig. 5 [44]. At lower temperatures, the compounds are solids and are relatively non-reactive; at moderately higher temperatures, they are decomposed to form non-corrosive solid products. At still higher temperatures the deposits are fluid and they strongly affect the metal sections. Variations in fuel and in methods of firing, affect the nature and rate of formation of deposits on superheaters.

Coal ash carried by the flue gas in the form of small particles from sintered and fused deposits on wall

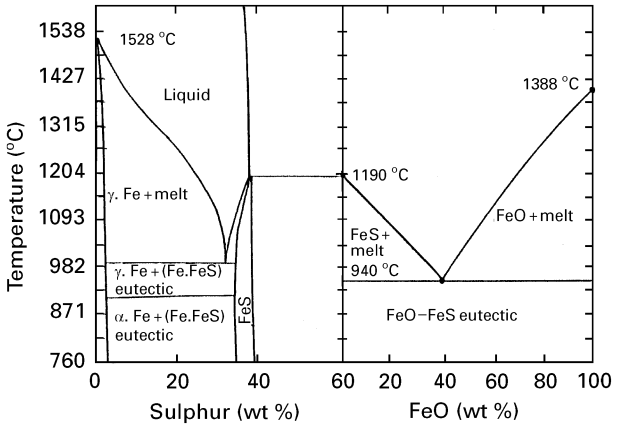

Figure 4 Phase diagram of the systems Fe–S and FeO–FeS.

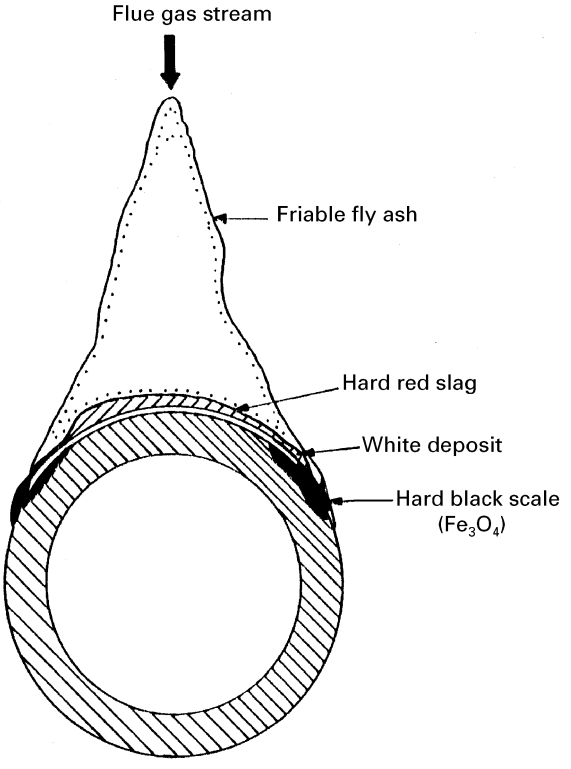

Figure 5 Deposit formation on a reheater element [44].

tubes, form slag deposits (birds nest) [45] and other similar accumulations on superheater and reheater surfaces. At temperatures down to about 922 K sintering can occur to bind loose ash particles into a moderately strong mass.

Alkali-matrix deposits, such as Na_2SO_4 present in the mass of fly ash collected on the tube surface can serve as the binding material for the remainder of the ash at temperatures as low as 1105 K. These build up into thick layers on superheaters and reheaters leading to three kinds of problems: (a) reduced heat transfer of the tube, (b) plugging of gas passages in severe cases and (c) providing the environment in which complex sulphates are formed causing metal wastages. These sintered ash deposits formed on boiler tubes and superheater tubes are usually of layered structure, because the main constituents of ash, such as silicates and sulphates, are immiscible. The layered structure is further enhanced by high porosity of sintered matrix and the temperature gradient of the ash material.

Like the alkali-matrix type, phosphatic deposits also are bonded but the bonding agent is a phosphorus compound rather than a sulphate. Phosphatic deposits seldom occur in pulverized coal fired units.

3.3. Air heaters

Air heaters are operated at lower temperatures and they do not lead to excessive corrosion and plugging. However, if the metal temperature is too low and the dew point is reached, sulphuric acid condenses and corrosion accelerates. Oxidation of metal components by flue gas at air-heater temperatures is insignificant, but the presence of a wet liquid film can cause catastrophic failure.

The relationship between the dew point and SO_3 concentration [46–48] is of great concern (Fig. 6) because the dew point establishes the minimum metal temperature to prevent condensation of a liquid acid film. The amount of acid that is not condensed and therefore passes through the condenser is a measure of the partial pressure of sulphuric acid at the temperature of the condenser. Hence it is also the concentration of sulphuric acid which is responsible for corrosion. Fig. 7 shows the relative amount of H_2SO_4 condensed on metal surfaces at different temperatures for various concentrations of acid in a stream of air containing 5 wt% water vapour [40]. It is of considerable interest to note that even 0.0001 wt% i.e., 1 ppm, of SO_3 in the air stream leads to appreciable condensation at temperatures as high as 388.5 K.

In summary deposit build up is affected by the trapping of the smallest dust particles by surface irregularities on plates, by the further capture on large particles by this first layer, and by the abrading action of the largest pieces of ash. In addition, chemical reactions occur at least to a limited extent, even above the dew point of the flue gas. Deposits accumulate most rapidly in colder sections and are characterized by particle solubility in water, the presence of sulphates, and low pH. Solubility in water ranges from 13–19%, the most soluble deposits occurring when the preheater plates are being attacked by acid. Sulphuric

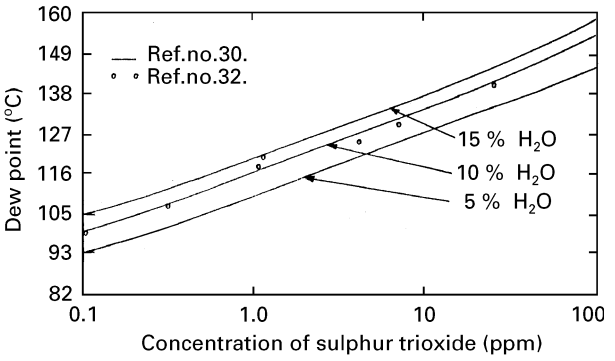

Figure 6 Dew point of SO_3 in flue gas [46].

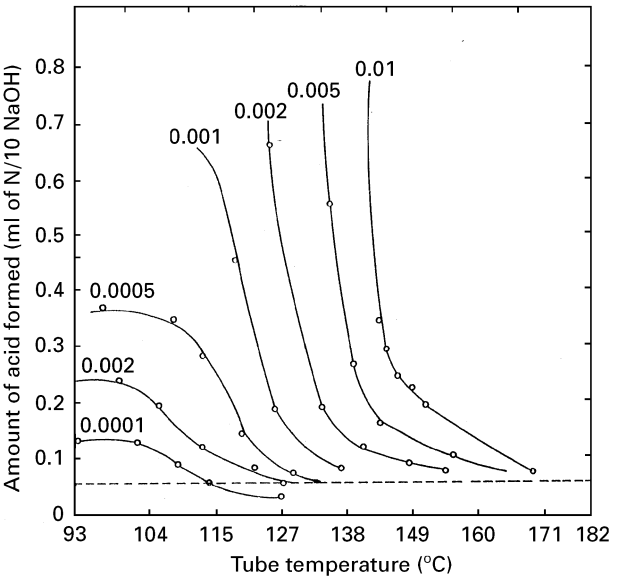

Figure 7 Relative amounts of sulphuric acid condensed on the tube metal surface [40].

acid is blamed mostly for loss of metal, and the rate at which the acid condensation occurs is more meaningful in relation to air-heater corrosion.

3.4. Cyclone burners

The expectation of freedom from superheater fouling, due to the low dust loading typical of a cyclone furnace, has unfortunately not been realized. This is because, in this case, each fly ash particle serves as a nucleus for condensation of alkalis. These alkalis then condense directly on relatively cool tube surfaces, allowing fly ash to subsequently adhere which, because of their fineness and low concentration, decrease any erosive action that would tend to scrub deposits from tube surfaces.

4. Mechanism

Metal loss in boilers is the result of various mechanisms and not exclusively of one set of chemical reactions. It is well known that the rate of oxidation is determined, like that of any other heterogeneous reaction, not so much by the rate of chemical reaction of the components as by diffusion through the oxide layer and by the reaction at the inter-faces [49]. For

example, wustite ($Fe_{1-\Delta}O$), magnetite ($Fe_{3+\delta}O_4$) and haematite ($Fe_{2+\varepsilon}O_3$) which are stable at high temperature (depending on temperature and oxygen activity) can very well become the reactants as well as the product of reactions. A dense magnetite layer may form as a result of oxidation of wustite to magnetite, reduction of haematite to magnetite, or the solid state reaction between wustite to haematite by the transport of iron and/or oxygen through the product layers of magnetite, by means of bulk diffusion, grain boundary diffusion or by gas diffusion along pores or cracks. In the case of a dense structure, diffusion along the grain boundaries, pores, cracks etc. is thought to be negligible, compared to that through cation vacancies and from interstitials. Fig. 8 illustrates the important solid phase reactions which determine the rate of oxidation [50], they can apparently be grouped into two basic categories i.e.,

(i) reactions in the scale film,
(ii) reactions at the phase boundary between scale and metallic substrate.

However, the extent of corrosion measured during funace outages, does not help in identifying the operating conditions responsible for metal loss. In addition metal and gas temperatures, and the composition of the flue gas and of deposits in corrosion areas, cannot be determined accurately because the normal variations in fuel characteristics and changing heat load are constantly affecting the environmental conditions throughout areas where corrosion can occur.

The glassy silicate and sulphate constituents of ash deposit on the boiler tubes form a slag matrix which strongly adheres to the metal surface. The strength of the adhesive bond formed between the oxide surface and ash deposit significantly depends on the characteristics of the oxide layer and the ash deposits. It may be noted that since there is no gross mismatch (or incompatibility) in their thermal expansion characteristics, the strongly bonded [51] deposits once formed on steel tubes are not easily dislodged on thermal cycling. However, ash deposits peel off the austenitic steel tubes on cooling, showing poor adhesion. Erosion from ash particles moving at high velocity can enhance corrosion and gas phase oxidation, by removal of the protective scale on metals through chemical reaction with a corrodent formed within an overlying deposit by reaction of the protective scale with constituents in the flue gas and the overlying deposit, by direct attack of the metal surface. Otherwise the presence of a liquid phase is a necessary criterion for corrosion reaction to take place at an appreciable rate.

Generally, corrosion reactions occur at a high rate, in the presence of liquid phase on the surface of a metal because a liquid phase provides an "electrolyte" for electrochemical attack.

The relative rate of oxidation in such reactions can be related to the electrode potential series in a solvent of alkali sulphates which is determined by the concentration of the dissolved metal, the amount of oxygen and sulphur oxides in the melt, and the possible presence of other substances such as chloride ions. Although boiler deposits usually show negligible amounts of chlorides, yet, experiments [52] with a synthetic flue gas containing HCl vapour showed that the morphology of the oxide layer (haematite) changed from that containing blisters and cracks, to porous and discontinuous, to complete disintegration as the HCl vapour was increased from 0.1–0.2–0.8 vol%. The degree of attack depends on the concentration of SO_3 in a molten sulphate on the surface of the metal [53], and the rate of dissociation of sulphate ions which probably etablishes the rate of corrosion.

$$SO_4^{2-} + 8e^- \rightarrow S^{2-} + 4O^{2-} \qquad (5)$$

(Sulphate and chloride ions behave similarly).

In addition the thickness of deposits probably depends on varying the SO_3 concentrations at the metal surface, which also creates a gradient in the corrosion potential, e.g., a macrogalvanic couple across a tubular section (Fig. 9) at a potential difference of 0.5 V between a metal in contact with solid sulphates at one point and fused sulphates at another [54]. This accounts for the observed greater loss of metal at the sides of tubes rather than those directly in line with the oncoming gas stream, where the deposit is thickest. Several studies have shown that the fire side corrosion of fludized-bed combustors in the form of accelerated oxidation, internal sulphidation and break-down of protective oxide layer. With nickel-base materials at temperatures close to bed temperatures, liquid nickel sulphide may form, leading to catastrophic attack

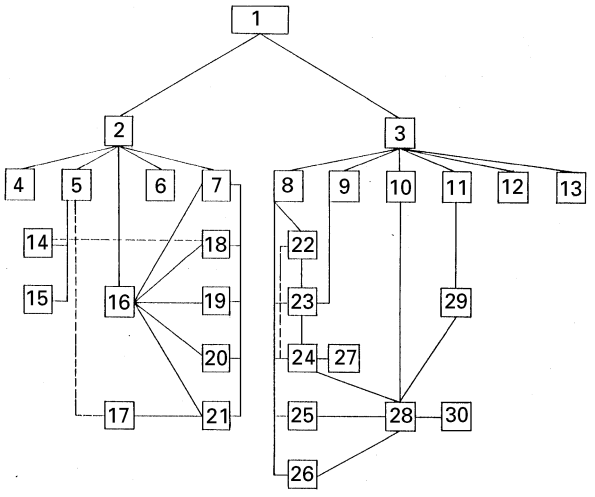

Figure 8 Effect of solid phase reactions on oxidation rate of metals and alloy [50]. (1) Solid-phase reactions; (2) reactions at interphase; (3) reactions in scale layer; (4) internal oxidation; (5) texture and orientation; (6) displacement reactions; (7) state of metal; (8) mutual solubility of oxides; (9) polymorphic transformations; (10) formation of phases with defective structure; (11) type n-p junction conductivity; (12) formation of spinels; (13) formation of low-melting eutectics; (14) effect of crystallographic orientation; (15) orientation and dimensional conformity; (16) electron emission; (17) oriented texture; (18) anisotropic distribution of nucleation centres; (19) lattice transformation; (20) magnetic transformations; (21) plastic deformation; (22) relation between ion radii; (23) lattice distortion; (24) stabilization of oxide phases; (25) valence ratio; (26) caking of scale; (27) stability of solid solution of oxides; (28) changes in concentration of lattice defects; (29) changes in the nature of defects; (30) changes in the colour of oxides.

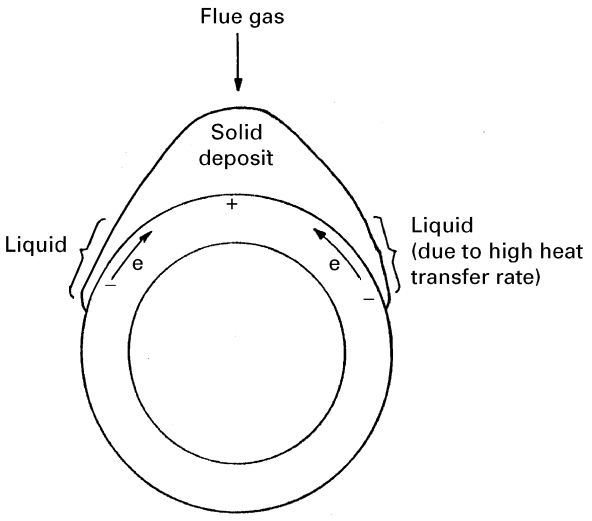

Figure 9 Macro-galvanic action across deposits on boiler tube [65].

[55]. The mechanism seems to depend on the reaction path, i.e., the formation of stable chromium sulphide below the chromium oxide layer, which actually prevents reestablishment of a Cr_2O_3 scale, once it is penetrated. Further, increased sulphur activity within the alloy, with concomittant depletion of chromium by oxidation, can result in nickel sulphide formation. A rapid oxidation can become catastrophic [56].

4.1. Scale growth

In superheaters and reheaters, ferritic alloys are observed to have only low temperature oxide phases: an inner layer of magnetite, Fe_3O_4 and an outer layer of haematite, Fe_2O_3. The haematite layer occurs at the oxide–steam interface as a thin and discontinuous layer and has very little effect on the oxidation rate [57]. The magnetite layer is the predominant phase; it exhibits a simple duplex morphology. In some cases, multiple laminations may form. The major morphology is a thick magnetite layer at the steam–scale interface paired with a thinner iron-chromium spinel layer; several pairs of thinner lamination between outer pair and the metal; and through scale cracks [58].

The scale-growth takes place by a diffusion-transport mechanism in which the dissociation of steam produces oxygen molecules which further dissociates into atoms that are then ionized into ions and then chemisorbed the necessary electrons being supplied by the metal, and are transported by diffusion through the oxide towards the oxide-steam interface. The chemisorbed oxygen ions are incorporated into a spinel structured lattice, forming a new layer of magnetite with a high concentration of metal defects. Thus, two layers of scale may grow from the original metal surface: one grows outwards and the other inwards. Both consist of magnetite, but the outer layer is rich in iron vacancies, while the inner one contains excess iron and oxygen vacancies. The inner layer also contains most of the alloying elements in steel. The boundary between inner and outer layer is usually porous (Fig. 11(a–c)).

Extensive studies on erosion-corrosion have been reported by Levy and others [59–61]. They have indicated that the impact of small solid particles on a steel erosion–corrosion specimen, increases the scale formation temperature, the scale being formed by the growth of nodules at locations where particle impacts have damaged the passivated scale layer. Subsequent scale growth is by consolidation of nodules or layered growth of scale in the areas from where the initial nodules are removed. At lower particle velocities, scales remain segmented and the mechanism is of slow chipping and cracking, whilst at higher velocities the scale is consolidated and wastage is due to a high rate microspalling mechanism. Angular particles result in higher erosion rates and the mechanism is different to that for round particles. High chromium steels were found to have lower metal wastage rates.

Wright [62] has presented a comprehensive review on high temperature erosion in coal combustion. Distinct regimes have been identified where solely erosion or corrosion, or synergestic effects or both are responsible for material loss. In erosion controlled regimes a simple relationship between resistance and the inverse of hardness appears to offer a reasonable basis for the selection of materials. Regimes involving combined effects have yet to be exhaustively investigated since the mechanisms are expected to be complex.

4.2. Pyrosulphate attack

If the temperature in the system is low and if there is an appreciable concentration of SO_3, a corrosion mechanism involving the formation of pyrosulphates can occur. The existence of this mechanism depends on the availability of high concentrations of SO_3 which is produced by the catalytic oxidation of SO_2 on active surfaces which can create SO_3 concentrations much higher than those found in bulk free gas [63]. For example, at least 10,000 ppm SO_3 must be present for $K_2S_2O_7$ to form at 811 K. However under the usually encountered conditions, even when a fuel containing 4–5% sulphur is burned, the SO_2 content in the flue gas will not exceed 3500 ppm; hence the maximum SO_3 that can be formed will still be only one tenth of that necessary to form the pyrosulphates at a superheater metal temperature of 866 K. At 811 K, the SO_3 available is still only a third of that necessary to form pyrosulphates.

Thus, a consistent mechanism for corrosion can be attributed to pyrosulphates only in the temperature range 672–755 K. In this lower temperature range, the mechanism can be straight forward [37] and consists of the deposition of alkalis on exposed metal surfaces followed by conversion of the alkalis to $Na_2S_2O_7$ and $K_2S_2O_7$ by reaction of sulphates with SO_3 and their reaction with oxide films on metal surfaces, according to the reactions;

$$3Na_2S_2O_7 + Fe_2O_3 \rightarrow 3Na_2SO_4 + Fe_2(SO_4)_3; \text{ or} \quad (6)$$

$$4Na_2S_2O_7 + Fe_3O_4 \rightarrow 4Na_2SO_4 + Fe_2(SO_4)_3 + FeSO_4 \quad (7)$$

or the alternate path:

$$3Na_2S_2O_7 + Fe_2O_3 \rightarrow 2Na_3Fe(SO_4)_3 \quad (8)$$

which then breaks down according to:

$$2Na_3Fe(SO_4)_3 \rightarrow 3Na_2SO_4 + Fe_2O_3 + 3SO_3 \quad (9)$$

Finally, further oxidation of the metal occurs in order to replace its surface oxide film, according to the reaction

$$3Fe + 2O_2 \rightarrow Fe_3O_4 \quad (10)$$

and the consequent metal loss.

4.3. Trisulphates

For metal loss in superheaters and reheaters, the alkali iron trisulphates $Na_3Fe(SO_4)_3$ and $K_3Fe(SO_4)_3$ are thought to be responsible rather than pyrosulphates [64–66]

$$2Fe_3O_4 + 9K_2SO_4 + 9SO_3 + 0.5O_2 \leftrightarrows 6K_3Fe(SO_4) \quad (11)$$

$$Fe_2O_3 + 3K_2SO_4 + 3SO_3 \leftrightarrows 2K_3Fe(SO_4)_3 \quad (12)$$

$$3Fe + 2O_2 \rightarrow Fe_3O_4 \quad (13)$$

$$4Fe + 3O_2 \rightarrow 2Fe_2O_3 \quad (14)$$

The iron oxide dissolved in these sulphates could have originated from the oxide layer on the boiler tube [66] (Fig. 10) or may have been extracted from the deposited ash.

The necessary steps involved may be categorized as follows:

(a) Presence of oxide film on the metal surface, as shown in Fig. 11(a – c).

(b) Deposition of alkali sulphates (originating from the alkalis in the fuel ash and the sulphur oxides in the furnace atmosphere) on the oxide layers. As an example this deposit could be K_2SO_4. The layer becomes sticky because of the increasing temperature gradient, so that the particles of fly ash are captured and heated to the point where SO_3 is released by thermal dissociation of sulphur compounds in the ash, and this SO_3 migrates towards the cooler metal surface. A layer of slag forms on the outer surface.

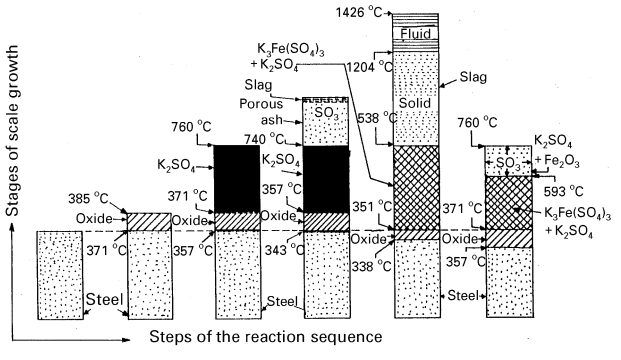

Figure 10 Formation of complex sulphates by removal of protective oxide film [66].

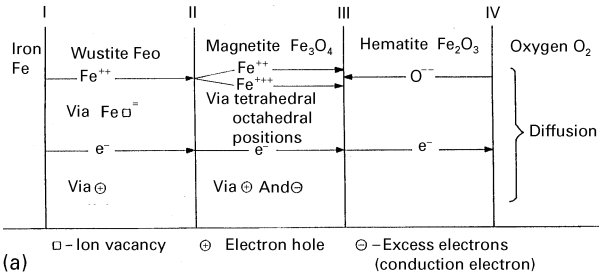

Phase boundary reactions:

I. Fe (metal phase) + $(Fe\square^{=} + 2\oplus)$IN FeO ⇋ Null

II. $Fe_3O_4 \leftrightharpoons (4FeO + Fe\square^{=} + 2\oplus)$IN FeO
(Fe_3O_4 decomposition)
Some of the Fe^{2+} ions arriving through the FeO phase and the Fe^{3+} ions arising at the FeO/Fe_3O_4 phase boundary pass over into the magnetic phase:
$\oplus_{IN\ FeO} + (Fe\square^{=} + Fe\square^{\equiv})$ vacant tetrahedral positions in $Fe_3O_4 \leftrightharpoons$ filled lattice positions + $(2Fe\square^{=})$IN FeO

III. $12\ Fe_2O_3 \leftrightharpoons 9Fe_3O_4 + (Fe\square^{=} + 2Fe\square^{\equiv} + 8\oplus)$
(Fe_2O_3 decomposition)
$2Fe_3O_4 \leftrightharpoons 3Fe_2O_3 + (O\square^{=} + 2\theta)$IN Fe_2O_3
(Fe_2O_3 formation)

IV. $1/2\,O_2(g) + (O\square^{=} + 2\theta)$IN $Fe_2O_3 \leftrightharpoons$ Null

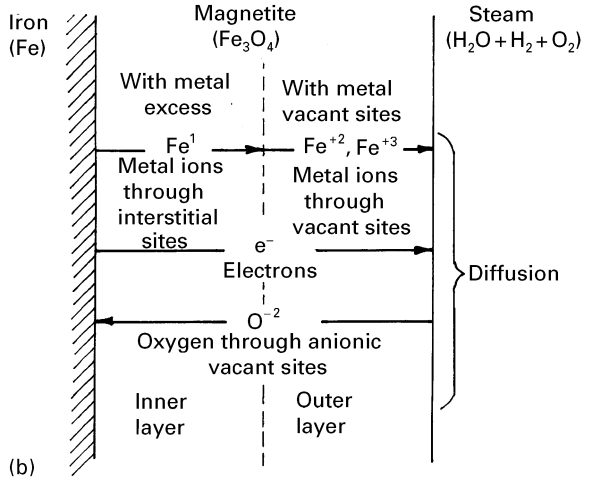

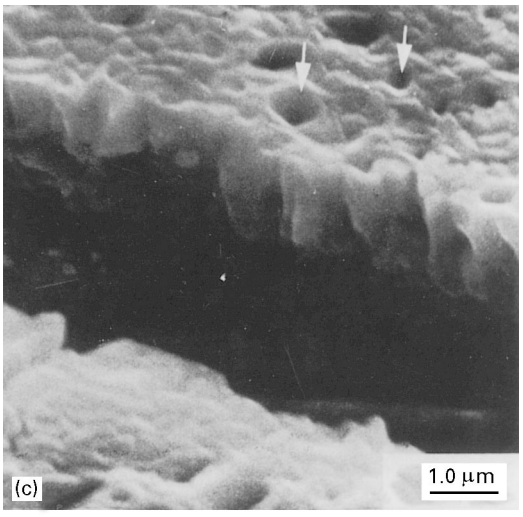

Figure 11 (a) Diffusion process and phase boundary reactions during oxidation of iron in oxygen [66]. (b) schematic representation of diffusion process by solid-state transport through scale during oxidation of iron and dilute alloys [58]. (c) fracture surface of superheater tube, in superheated steam during early stage of scale growth. The arrows indicate pores emerging from outer surface of scale [58].

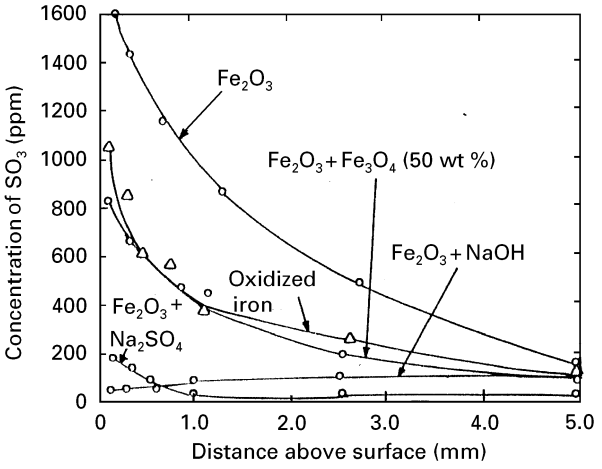

Figure 12 Levels of SO_3 existing over Fe_2O_3 surface (gas-stream velocity 1.2 ft s^{-1} [67].

(c) If the temperature in the deposited layer falls, the oxide scale may react with the SO_3 to form $K_3Fe(SO_4)_3$. This means the removal of the oxide scale and hence further oxidation.

(d) De-slagging may occur, exposing the $K_3Fe(SO_4)_3$ layer to temperatures high enough to dissociate it in part, releasing some SO_3 which moves towards the cooler part of the deposit, where it reacts with any K_2SO_4 still present and forms an additional amount of $K_3Fe(SO_4)_3$. Therefore, further oxidation of the metal occurs to provide the normal equilibrium thickness of scale.

This model, however, fails to identify the source of the SO_3 required to form the trisulphate (at least 250 ppm) at these temperatures. Yet another model indicates (Fig. 12) that the protected environment below a deposited layer can lead to nearly equilibrium concentrations of SO_3 by catalytic oxidation of SO_2 and provide ample SO_3 to take care of steps (b) and (d). The residence time of the flue gas in contact with the catalytically active surface could provide an essentially equilibrium concentration of SO_3 which could exceed 2000 ppm SO_3, which favours the formation of trisulphate [67].

The exposure of 18Cr–8Ni, Ti-stabilized steel specimens [36] to synthetic alkali iron trisulphates for 100 h confirmed that serious loss of metal can occur due to molten trisulphates at a high rate, and that the rate ceases above 977 K, where trisulphate is unstable (Fig. 13a) [36]. The trisulphate reacts with the metallic iron of the tube [65] to form K_2SO_4, Fe_2O_3, and FeS and the cycle is repeated. In this way, small amounts of alkali sulphates might lead to extensive loss of metal. The corrosive tendency of boiler deposits can be related to the ratio of potassium to sodium in the sulphate [68, 69]. A ratio of 5:1 or 7:1 has been observed in a highly corrosive deposit, whereas for a marginally corrosive deposit the ratio was 0.6:1 and 1.5:1. Another characteristic of highly corrosive potassium containing deposits is that they contain aluminium and iron in the form of complex sulphates. It should be noted that the thermal stability of potassium sulphate is almost 100 K higher than that of the

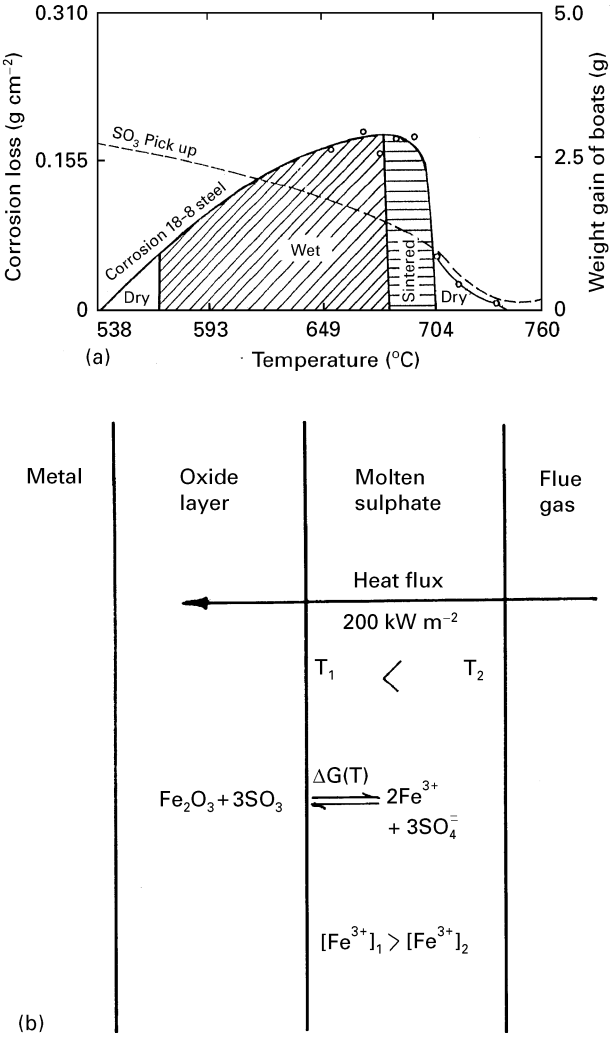

Figure 13 (a) Effect of molten trisulphate on corrosion [36] and (b) the mechanism of corrosion in molten sulphate [79].

sodium sulphate system. With respect to corrosion, the sulphate-rich deposits provide a good system for transport of ionic species in the melt, i.e., transport of metal ions (Fe^{3+} and Cr^{3+}) and oxidants (SO^{2-} and O^{2-}), and the rate of corrosion shows an exponential increase with temperature.

4.4. Sulphide formation

The direct reaction of the trisulphates with metallic iron or of the un-burned pyrites in the coal with the tube surface, or a reaction involving sulphur and the present metal (the elemental sulphur coming from the pyrites), may result in formation of massive amounts of FeS is corroded areas. Extensive studies on the problems concerning the removal of scales from steels heated in sulphurous atmospheres have found that the presence of SO_2 causes increased scaling rates (the effect being greatest in 'neutral' atmospheres). Also any addition of oxygen to these atmospheres generally reduces the effect of SO_2 (the sulphur partial pressure of the atmosphere is very sensitive to oxygen partial pressure and in the presence of 1 vol% SO_2 at 1073 K only 1 ppm oxygen is required to suppress the sulphur partial pressure to about 1.013×10^{-15} Pa). These conclusions have been amply demonstrated by the

increased reaction rate with gas flow rate up to a critical value that increases with temperatures and also by the presence of sulphides in the scale (mainly at the metal-scale interface). The highest rates are generally associated with the formation of liquid phases. It has been established [70–72] that the eutectic temperatures in the Fe–O–S system are Fe–FeS at 1253 K, FeO–FeS at 1213 K and Fe–FeO–FeS at 1138 K.

Sulphides and oxides have been observed to form together at the scale–gas interface under bulk atmosphere conditions [73, 74]. This indicates that the conditions at the scale–gas interface need not be representative of the bulk atmosphere, and the diffusion processes through the scale are very rapid. Duplex scales observed in the cases of iron [75–77] and nickel [78] provide a mechanism for very rapid ionic transport through the scale, particularly if the sulphide is present as a continuous network through out the scale.

The mechanism requires a highly conductive sulphide path to maintain a high metal activity at the reaction site which in turn produces high sulphur partial pressures causing further sulphide formation (Fig. 13b) [79]. Under controlled oxidizing atmospheres, a layer of oxide begins to form at the scale–gas interface and sulphide formation is suppressed at that site. The reaction rate is then controlled by diffusion of ions through the outer oxide layer and rapidly assumes parabolic type kinetics. This gives a possible explanation for the occurrence of two rate constants K_I and K_{II} during sulphidation of 310 stainless steel. Initially the mixed spinel reduces the sulphur potential at the scale–alloy interface which is indicated by the dissociation pressure of mixed spinel. The dissociation pressure is also a function of the activity of FeS in the mixed spinel and consequently becomes a function of the sulphur pressure at which the reaction is carried out. The parabolic rate constants yield similar variations with respect to sulphur pressures and suggest that the diffusing species over the entire range of sulphidation is identical. However, the protective surface layer has been shown to suffer a cyclic variation in corrosion rate as a typical feature [80]. This is due to the temperature gradient across the molten sulphate layer on superheater tube which causes a concentration gradient of the metal sulphate (Fig. 13b) [79] and results in continued dissolution of the protective oxide in the interfacial region between the molten sulphate layer and the porous ash deposit.

The morphology of duplex scales formed on iron-base alloys has been discussed in detail in the literature [81–88]. It is suggested that the growth of a compact single layer of FeS scale, during the initial short period of sulphidation, is due to an outward diffusion of Fe^{++} ions towards the scale/sulphur interface, while the vacancies flow simultaneously in the opposite direction and are injected into the alloy surface (Fig. 14). Many of the iron-base and nickel-base alloys for high temperature service contain aluminium. A reduced rate of sulphidation has been observed in such alloys with the creation of localized strain-fields in the FeS lattice due to $A1^{++}$ incorporation. The continued injection of vacancies eventually leads to the formation of voids [86, 89]. In the region

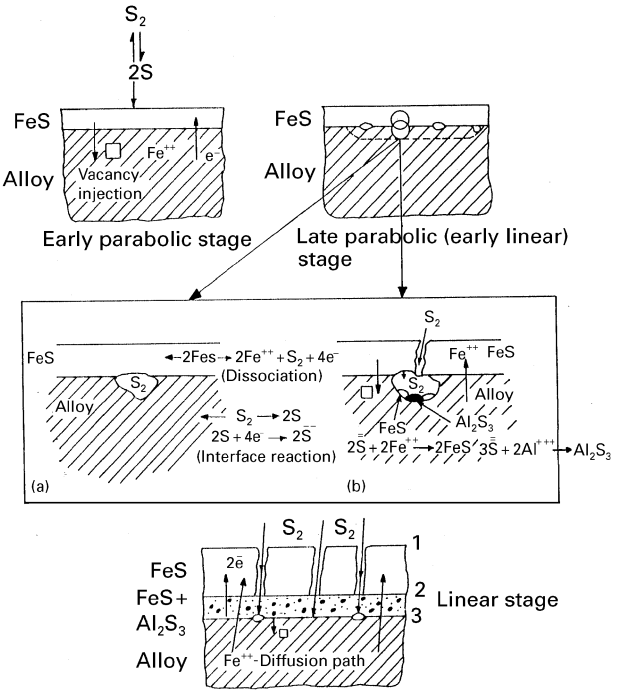

Figure 14 Dissociation reaction and vacancy incorporation mechanism [83].

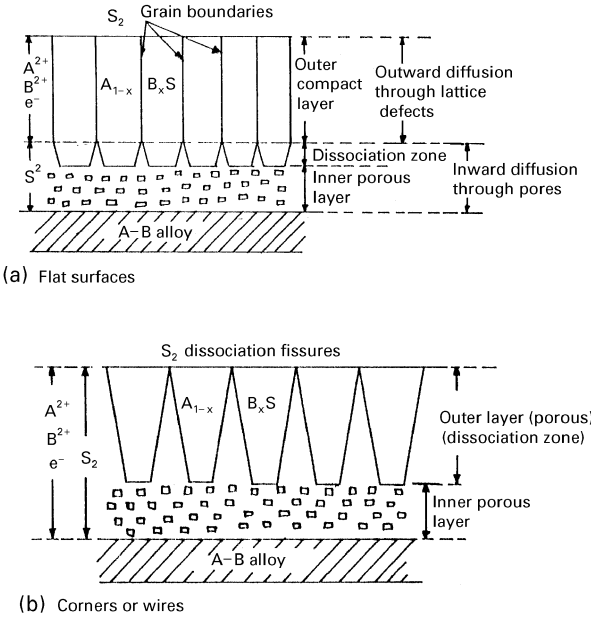

Figure 15 Essential difference in the mechanism of scale formation in the vicinity of (a) flat surface and (b) edges [90].

of these voids FeS dissociates to produce sulphur vapour which reacts with the underlying alloy, allowing heterogeneous nucleation and growth of the inner layer of FeS and Al_2S_3. The growth of this inner layer may prevail via a dissociation mechanism, i.e., the rate of incorporation of a vacancy in the alloy. In the case of Fe–Ni type of alloys [90], it has been observed that the mechanism of scale growth on the same sample of the alloy is essentially different in the vicinity of the edges and on flat surfaces (Fig. 15).

Sulphidation of ternary and multicomponent alloys is a complicated phenomenon. The scale formed on such alloys is composed of several phases and often

consists of several layers. In analogy with the case of binary Fe–Cr alloys, the scale formed on Fe–Cr–Al alloys is composed of four layers [91], the main two of which are; outer (I) and inner (II) layers. These are compact and are formed by outward diffusion of the alloy components (Fig. 16). The outer layer of the scale consists of ferrous sulphide doped with aluminium and the other inner layers consist of a mixed sulphospinel of general formula: $Fe(Fe_xAl_yCr_{2-x-y})S_4$.

In ternary Ni–Cr–X alloys [92] (X = Zr, Sm, La, Ce, Th, U, Y, V) as shown schematically in Figs. 17 and 18 a homogeneous scale [solid solution of general formula $(Cr, X)_xS_y$] is formed in competition with sub-scaling depending on the characteristics of the element X. This sometimes becomes impervious and practically stops the sub-scaling. In such alloys, therefore, single or double-phase scales are observed. For instance, at a sufficiently low content of the less noble alloying addition, a single phase scale consisting of either pure sulphide of the base material or of dilute solid solution of sulphides of both alloy components is formed. When the concentration of the less noble alloying component is sufficiently high, then a single phase scale consisting of pure sulphide or of sulphide doped with the component of doped material is formed.

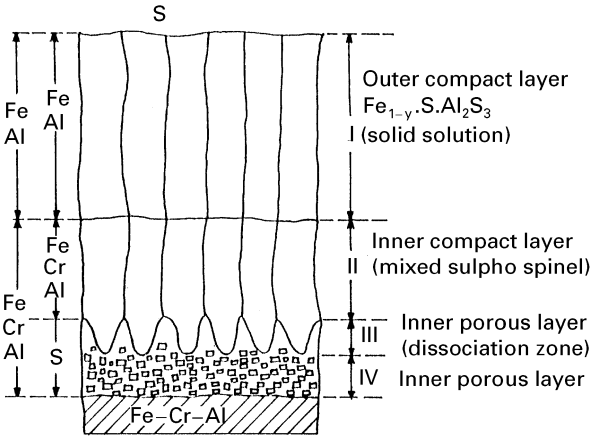

Figure 16 Model of the multilayer sulphide scale growth of Fe–Cr–Al alloys [91].

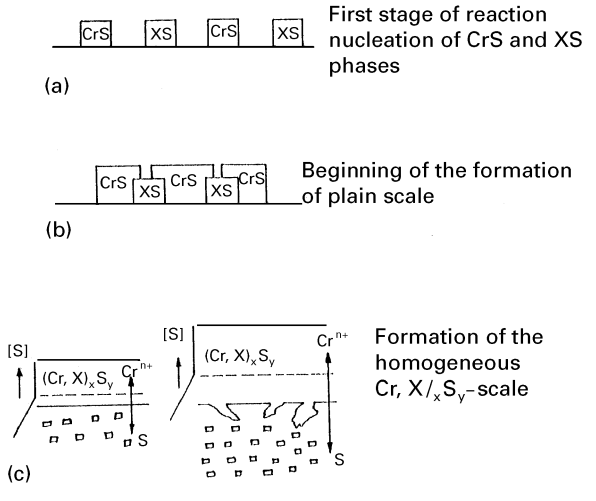

Figure 17 Model of the multilayer sulphide scale growth on Ni–Cr–X alloys [92].

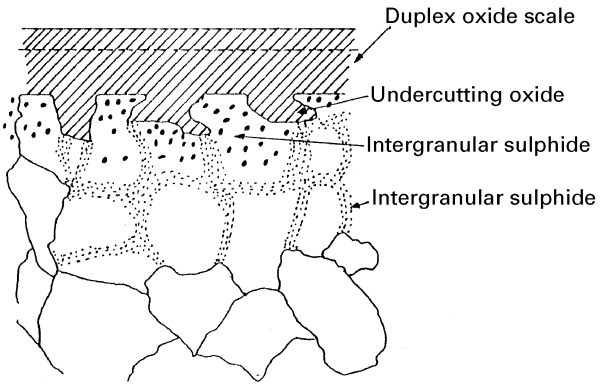

Figure 18 Corrosion features in O_2/SO_2 environment, 24 h exposure (Ni–Cr–X alloy) [94].

The effects of the addition of a rare earth element on the breakdown of protective oxide scales has been discussed in the literature [10, 93–95]. It is reported that the scale breakdown for a Fe–25Cr alloy is initiated at the scale/gas interface with the formation of FeS. The continued growth of the sulphide presumably proceeds inwards towards the scale/metal interface. Extensive studies on external and internal sulphidation of ferritic and austenitic steels after preoxidation have been reported in the literature [4, 96–99]. These indicate that the scale on chromia may fail at high temperature in oxidizing–sulphidizing atmospheres by external or internal sulphidation. After preoxidizing the alloys at 1173 K the subsequent exposure to an H_2–H_2O–H_2S atmosphere at 973 K leads to extensive production of FeS on top of the Cr_2O_3 layer in the austenitic alloy and the formation of small fringes of Cr_3S_4 on the chromia layer in the ferritic alloy.

The kinetic mechanism of sulphidation of metals and alloys can be explained, using the currently available data base. They follow a parabolic rate law, of which the slowest contributing process, which determines the overall rate of the corrosion, is the diffusion of the reagent in the scale. The majority of metal sulphides only exhibit a defect structure on the cation sublattice, and hence the growth of compact scales takes place by outward diffusion of metal ions.

5. Conclusion

The presence of inorganic minerals in the fuel, leads to severe wastage of metallic bodies in power generating installations. When the coal is burned, the minerals are converted into ash, clinker, slag and fly-ash. Amongst the various corrosive particulates, sulphur assumes a predominant role existing in the elemental form and also as complex pyrosulphates, trisulphates, oxides, etc. In addition the competitive role of partial pressure of sulphur and oxygen has been attributed to the occurrence of sub-scale precipitation.

However, the exact mechanism of oxidative attack by either an aggresive gaseous environment or by several complex chemicals formed from ashes, deposit by-products or corrosion products, are unclear due to difficulties involved in duplicating and understanding

the reactions going on *in-situ*. The multilayer growth of scales and other morphological characteristics have been understood in terms of distributions of the alloying elements and the base metal.

Several attempts have been made in the past to unravel the basic reaction sequence from the laboratory and industrial data available in the literature. However, the analysis of failed components and systematic data collection are still the only realistic methods of studying the corrosive attack of metallic components in service under high temperature power generating conditions.

The deposit-enhanced high temperature corrosion of tube metals has been discussed. A deterioration of the protective oxide scales due to thermal and chemical activity of deposits, accompanied with erosion and wear has been shown to have a major role in metal wastage.

References

1. P. KRATINA and J. MCMILLAN , "Fly-ash Erosion in Utility Boilers – Prediction and Protection", presented at the Canadian Electrical Association Conference, Regina, Sask., October 1982.
2. T. FLATLEY, E. P. LATHAM and C. W. MORRIS, *Mater. Perform.* **20** (1981) 12.
3. V. R. SUBRAMANIAN and R. R. GOPAL, in Proceedings of National Seminar on Materials of Thermal Power Plant, Bhopal, India (1994), p. 74.
4. G. H. MEIER, F. S. PETTIT and N. BIRKS, in "High Temperature Oxidation and Sulphidation Processes", edited by J. D. Embury (Pergamon Press, 1990), pp. 1–11.
5. T. NARITA, *Ibid* pp. 70–81.
6. T. NARITA and K. NISHIDA, in Proc. of 3rd Foundary J1.IIM' Symp. Trans. Jpn Institute of Metals **24**, 457 (1983).
7. T. NARITA and T. ISHIKAWA, *Mater. Sci. and Engng.* **87** (1987) 51.
8. *Idem*, in Proceedings of Symposium on High Temp. Mat. Chem., *Electrochem Soc. Japan*, **88** (1988) 71.
9. *Idem*, *Mater. Sci. and Engng.* **89** (1989) 31.
10. V. SRINIVASAN and D. E. GOODMAN, in "Corrosion and Particle Erosion at High Temperatures", edited by V. Srinivasan and K. Vedula (TMS, PA, 1989), pp. 178–89.
11. D. B. MENDOWCROFT and M. I. MANNING, eds. "Resistant Materials for Coal Conversion", (Elsevier, New York 1989).
12. J. F. NORTON, ed. "High Temperature Corrosion in Coal Gasification Atmosphere (Elsevier, New York 1984).
13. M. F. ROTHMAN, ed. "High Temperature Corrosion in Engineering Systems" (AIME, NY 1985).
14. M. SCHULTZ, *Oxidation of Metals* **8** (1986) 409.
15. M. UZ and O. N. CARLSON, *J. Less Comm Met* **79** (1981) 409.
16. *Idem*, *ibid*, **116** (1986) 317.
17. G. SARKAR , S. SAKHA, K. P. DASCHOWDHURY , S. K. HAZRA and S. K. SEN, Proceedings of the Ninth International Coal Preparation Congress, edited by Indian Coal Committee (New Delhi, India, 1982) pp. G. 1–13.
18. J. D. WATT, *B. C. U. R. A. Monthly Bul.* **49** (1982) 23.
19. A. R. POWELL, *Ind. Engng. Chem.* **12** (1920) 1069.
20. R. C. CONEY, H. A. GRABOWSKI and B. T. CROSS, *Trans. Amer. Soc. Mech. Eng.* **71** (1949) 951.
21. M. T. MACKOWSKY, *Femerungstechnik* **31** (1943) 143.
22. P. F. KERR and J. L. KULP, *Amer. Min.* **33** (1948) 387.
23. W. G. MARSKELL, J. M. MILLER and J. E. RAYNER, *Fuel* **25** (1946) 100.
24. W. OELSEN and H. MAETZ, *Mitt. Kaiser with Inst. Eisen Dusseldorf* **21** (1936)
25. W. L. BEDWELL, Royal Inst. Chem. Monograph No. 9 (1952)
26. H. E. CROSSLEY, *J. Inst. Fuel* **25** (1952) 221.
27. N. S. BORNSTEIN and M. A. DECRESCENT, *Trans. AIME* **245** (1963) 583.
28. *Idem*, *Metall. Trans.* **2** (1971) 2875.
29. J. A. GOEBEL and F. S. PETTIT, *ibid* **1** (1970) 1943.
30. J. A. GOEBEL, F. S. PETTIT and G. W. GOWARD, *Ibid* **4** (1973) 261.
31. A. LEVY and E. L. MERRYMAN, *Combust. Flame* **9** (1965) 229.
32. J. M. QUETS and W. H. DRESHER, *J. Mater.* **4** (1969) 583.
33. R. A. RAPP and K. S. GOTO, The Hot Corrosion of Metals by Molten Salts, Symposium on Fused Salts, 1978 (The Electrochemical Society, Princeton, NJ, 1979).
34. H. KRISCH , "Corrosion in Combustion Chambers Caused by Slag Attack and Flue Gases of Varying Composition" in Proceedings of Conference Mechanism of Corrosion by Fuel Impurities, Marchwood, UK, 1963 (Butterworth, London, 1963), p. 508.
35. H. E. CROSSLEY, *J. Inst. Fuel* **40** (1967) 342.
36. C. CAIM JR. and W. NELSON, *Trans. ASME J. Eng. Power* **83** (1961) 468.
37. P. M. BRISTER and M. N. BRESSLER, "Long-term Experience with Steel and Alloy Superheater Tubes in Power Boiler Services", Joint Conference on Creep, Institute of Mechanical Engineers, **1** (1963) 7.
38. R. W. EVANS and B. WILSHIRE, *Proc. Inst. of Met. London* (1985) 314.
39. R. VISWNATHAN , "Damage Mechanism and Life Assessment of High Temperature Components", *ASM* (1989) 229.
40. J. R. RYLANDS and J. R. JENKINSON, *J. Inst. Fuel* **27** (1954) 299.
41. C. J. SLUNDER, A. M. HALL and J. H. JACKSON, *Trans. ASME* **75** (1953) 1015.
42. A. B. HEADLEY, T. D. BROWN and A. SHUTTLE WORTH, ASME, No. 65-WA/CD-4 (1965).
43. E. RAASK, *Power Ind. Res.* **1** (1981) 233.
44. W. NELSON and C. CAIN JR., *Trans. ASME, J. Eng. Power* **82** (1960) 194.
45. H. E. CROSSLEY, "Fuel and the future", (H. M. Stationery office, London 1948) 36.
46. P. MULER,*Chem. Eng. Tech.* **31** (1959) 345.
47. H. GOKOSOYER and K. ROSS, Shell Res. Ltd., Thoronton Res. Centre Report, M (1962) 218.
48. E. S. LISLE and J. D. SENSENBAUGH, *Combustion* **36** (1965) 12.
49. C. WAGNER, *Z. Phys. Chem.* **21B** (1933) 25.
50. R. F. VOITOVICH and E. I. GOLOVKO, Proc. III ICMC, NACE (Canada) **4**, (1966) p 81.
51. A. K. MOZA, K. SHOJ and L. G. AUSTIN, *J. Inst. Fuel* **53** (1980) 17.
52. P. MAYER and A. V. MANOLESCU, Influence of HCl on Corr. of Boiler Steel in Synthetic Flue gas Corr. NACE, **36** (1980) 369.
53. B. W. BURROWS and G. J. HILLS, *Jl. Inst. Fuel* **39**, (1966) 168.
54. M. J. FOUNTAIN, *ibid* 178.
55. J. STRINGER, Materials Selection for In-Bed Components in Fludized Bed Combusion Systems, paper presented to the DOE/WVU Conference on Fludized Bed Combusiont, Morgantown, West Virginia, October 1980.
56. *Idem*, High Temperature Corrosion in Mixed Gaseous Oxidants in metals and Energy, Proceedings of the 33rd Annual Conference of the Australasian Inst. of Metals, Auckland, New England, May 1980, pp. 143–46.
57. P. J. GROBNER, C. C. CLARKE, P. V. ANDREAE and W. R. SYLVESTER, Steam-side Oxidation and Exfoliation of Cr-Mo Superheater and Reheater Steels, paper No. 172 presented at Corrosion 80, a NACE Conference, Chicago, March 1980.
58. P. MAYER and A. V. MANOLSEU, in Proceedings of High Temperature Corrosion, NACE-6, Conference held at San Diego, CA, March 1981, edited by R. A. Rapp (1983), p. 368.
59. A. V. LEVY , WEAR-Elsevier Publication, Switzerland, **108** (1) (1986) 1.

60. A. V. LEVY and E. SLAMOVICH, *ibid*, **110** (2) (1986) 117.
61. A. V. LEVY and Y. F. MAN, *ibid*, **111** (2) (1986) 135.
62. I. G. WRIGHT, *Mater. Sci. & Engng.* **88** (1987) 261.
63. D. A. SHORES and W. C. FRANG, *J. Electrochem Soc.* **128** (1981) 346.
64. W. T. REID, "External corrosion and Deposits" (Elsevier, New York 1971).
65. A. HENDRY and D. J. LEES, *Corrosion Sci.* **20** (1980) 383.
66. R. C. CONEY, B. J. CROSS and W. T. REID, *Trans. ASME* **67** (1945) 289.
67. H. H. KRAUSE, A. LEVY, and W. T. REID, *Trans. ASME, J. Engng. Power* **90** (1961) A38.
68. C. H. ANDERSON and C. W. GODDARD, *J. Inst. Fuel* **41** (1968) 357.
69. A. J. BLAZEWIPZ and M. GOLD, ASME haper 79, WA/FH-6 (1979).
70. D. C. HILTY and W. CRAFTES, *Trans. AIME* **194** (1952) 1307.
71. R. VOGEL and W. FULLING, *Festschriften, J. Arvid, Hedrall* (1948) 597.
72. T. ROSEUQUIST, *JISI* **176** (1954) 37.
73. F. S. PETTIT, J. A. GOEBEL and G. W. GOWARD, *Corrosion Sci.* **9** (1969) 903.
74. N. BIRKS, Oxidation of Metals in Atmospheres containing the Oxidants, in "High Temperature Gas-Metal Reactions in Mixed Environments", edited by Z. A. Doroulis and S. Janssen (AIME-TMS, Boston, 1973), p. 322.
75. A. RAHMEL and J. A. GONZALEZ, *Werkstoffe und Korrosion* **21** (1970) 925.
76. *Ibid* **22** (1971) 283.
77. T. FLATLEY, and N. BIRKS, *JISI* **209** (1971) 523.
78. M. R. WOOTON, and N. BRIKS, *Corrosion Sci.* **12** (1972) 829.
79. E. RAASK, "Mineral Impurities in Coal Combination", (Hemisphere, New York 1985) p 326.
80. A. J. B. CUTLER and E. RAASK, *Corrosion Sci.* **21** (1981) 789.
81. K. N. STRAFFORD and R. MANIFOLD, in Proceedings of the 4th Int. Cong. on Metallic Corr. NACE, Houston, Texas (1972) 249.
82. K. HAFFE and A. RAHMEL, *Z. Physik. Chem.* **199** (1952) 152.
83. P. V. GELD and A. K. KRASOVSKAYA, *Zhur. Fiz. Khim* **34** (1960) 1585, 1721.
84. A. RAHMEL, *J. Electrochem. Soc.* **107** (1960) 264.
85. W. D. KINGERY, ed. Kinetics Of High Temperature Processes (John Wiley, New York, 1959) p 97.
86. A. BRUCKMAN,*Corrosion Science* **7** (1967) 51.
87. C. WAGNER, *J. Electrochem. Soc.* **103** (1956) 627.
88. S. MROWEC *Roczniki Chem.* **34** (1960) 337.
89. I. A. MENZIES and K. N. STRAFFORD, *J. Mater. Sci.* **2** (1967) 358.
90. S. MROWEC, in Proceedings of symp. on properties of high temp. alloys edited by Z. A. FOROULIS and F. S. PETTIT (Electrochemical Soc. USA 1977) P413.
91. S. MORWEC and M. WEDRYCHOWSKA, *Oxidation of Metals* **13** (1979) 481.
92. K. N. STRAFFORD and J. M. HARRISON, in Proceedings of Int. Symp. on metals-slag-gas reactions and processes, Toronto, May 11–16, (1975) edited by Z. A. Foroulis and W. W. Smeltzer, p 464.
93. K. NATESAN, *Corrosion* **41** (1985) 646.
94. R. A. PERKINS, W. L. COONS and S. J. VORK, EPRI report (1982) ES-2452.
95. D. P. WHITTLE and J. SRINGER, *Phil. Trans Roy Sco.* **A 295** (1980) 309.
96. R. A. PERKINS, High temp corrosion – Ed. R. A. Repp, NACE-6, Texas (1983).
97. D. J. BAUTER, *Corrosion Science* **26** (1987) 153.
98. *Idem, Oxidation of Metals* **24** (1985) 331.
99. H. J. GRABKE, "Selected Topics of High Temperature Chemistry" (Elsevier, UK, 1989) p. 263.

Received 10 March 1995
and accepted 28 June 1996